Check for updates

Biotechnology and Bioengineering

WILEY

BIOTECHNOLOGY AND BIOENGINEERING

ARTICLE OPEN ACCESS

Mesenchymal Stem Cells-Derived Small Extracellular Vesicles and Their Validation as a Promising Treatment for Chondrosarcoma in a 3D Model in Vitro

Eugenia Romano[1,2] | Francesca Perut[3] | Sofia Avnet[4] | Gemma Di Pompo[3] | Simona Silvestri[1,2,5] | Felicia Roffo[1,2] | Nicola Baldini[3,4] | Paolo Antonio Netti[1,2,5] | Enza Torino[1,2,5]

[1]Interdisciplinary Research Centre on Biomaterials (CRIB), University of Naples Federico II, Naples, Italy | [2]Department of Chemical, Materials and Production Engineering (DICMaPI), University of Naples Federico II, Naples, Italy | [3]Biomedical Science and Technologies and Nanobiotechnology Laboratory, IRCCS Istituto Ortopedico Rizzoli, Bologna, Italy | [4]Department of Biomedical and Neuromotor Sciences, University of Bologna, Bologna, Italy | [5]Fondazione Istituto Italiano di Tecnologia, IIT, Naples, Italy

Correspondence: Enza Torino (enza.torino@unina.it)

Received: 30 July 2024 | **Revised:** 25 November 2024 | **Accepted:** 2 December 2024

Keywords: 3D tumor models | chondrosarcoma | drug carriers | extracellular vesicles | high-pressure homogenization | spheroids

ABSTRACT

Chondrosarcomas (CHS) constitute approximately 20% of all primary malignant bone tumors, characterized by a slow growth rate with initial manifestation of few signs and symptoms. These malignant cartilaginous neoplasms, particularly those with dedifferentiated histological subtypes, pose significant therapeutic challenges, as they exhibit high resistance to both radiation and chemotherapy. Ranging from relatively benign, low-grade tumors (grade I) to aggressive high-grade tumors with the potential for lung metastases and a grim prognosis, there is a critical need for innovative diagnostic and therapeutic approaches, particularly for patients with more aggressive forms. Herein, small extracellular vesicles (sEVs) derived from mesenchymal stem cells are presented as an efficient nanodelivery tool to enhance drug penetration in an in vitro 3D model of CHS. Employing high-pressure homogenization (HPH), we achieved unprecedented encapsulation efficiency of doxorubicin (DXR) in sEVs derived from mesenchymal stem cells (MSC-EVs). Subsequently, a comparative analysis between free DXR and MSC-EVs encapsulated with DXR (DXR-MSC-EVs) was conducted to assess their penetration and uptake efficacy in the 3D model. The results unveiled a higher incidence of necrotic cells and a more pronounced toxic effect with DXR-MSC-EVs compared to DXR alone. This underscores the remarkable ability of MSC-EVs to deliver drugs in complex environments, highlighting their potential application in the treatment of aggressive CHS.

1 | Introduction

Chondrosarcomas (CHS) are malignant bone tumors formed by cartilage-producing cancer cells (Donati and Bianchi 2020). They rank as the third most prevalent primary malignancies of the bone, trailing behind Ewing sarcoma and osteosarcoma. CHS account for 20%–27% of all primary malignant osseous neoplasms (Kim et al. 2020).

CHS are a quite heterogeneous group of cancers, and their clinical behavior and prognosis largely depend on tumor grade. High-grade CHS (II and III) often develop lung metastases and have a worse prognosis than low-grade tumors (Nazeri et al. 2018).

Surgery stands as the primary treatment for majority of CHS, given the limited efficacy of conventional chemotherapeutics. Notably, CHS exhibit high resistant to both chemotherapy and radiotherapy, likely attributable to factors such as the elevated concentration of the extracellular matrix, low percentage of dividing cells, and poor vascularity (Simard et al. 2017). In most instances, CHS carry a favorable prognosis, attributed to

This is an open access article under the terms of the Creative Commons Attribution-NonCommercial License, which permits use, distribution and reproduction in any medium, provided the original work is properly cited and is not used for commercial purposes.

© 2024 The Author(s). *Biotechnology and Bioengineering* published by Wiley Periodicals LLC.

indolent growth and rare metastases, when treated appropriately with surgery. The reported relative 5-year survival rate for CHS stands at 75.2%, although it significantly diminishes for high-grade tumors, especially for the dedifferentiated histological subtype (11%–24%) (Zając et al. 2021). Consequently, the imperative to explore novel therapeutic modalities becomes crucial, particularly for these more aggressive cases.

In this scenario, nanomedicine, mainly represented by inorganic (Sha et al. 2013; Pieretti et al. 2020), polymeric (Shield et al. 2020), and lipid nanoparticles (Trucco et al. 2018), is emerging as an advanced option for treating CHS, as it offers several advantages for drug delivery and cancer targeting (Kim et al. 2020). However, few studies on vesicles have been reported, and mostly limited on the evaluation of in vitro cytotoxicity of nanocarriers in CHS 2D SW1353 models (Tudor et al. 2023; Chongchai et al. 2024; Guan et al. 2024).

Despite the promising results in targeting cancer cells, immunogenicity and toxicity remain significant issues associated with these nanovectors (Kim et al. 2020). Therefore, in recent decades, small extracellular vesicles (sEVs) have emerged as a novel alternative due to their diverse properties (Jafari et al. 2020; Yan et al. 2023; Tong et al. 2023). Their composition and unique architecture facilitate crossing various natural barriers, intercellular communication, and organ tropism. At the same time, the lipid membrane protects the complex inner cargo from degradation in the bloodstream (Elliott and He 2021).

Among these natural nanocarriers, mesenchymal derived extracellular vesicles (MSC-EVs) have gained significant interest for their therapeutic potential (Sun et al. 2021). Although the functional mechanisms of MSC-EVs are not fully understood, and the number of reports is limited, they have shown the ability to mirror the phenotype of parent mesenchymal stem cells (MSCs), providing therapeutic effects such as regeneration of tissue injuries, suppression of inflammatory responses, and modulation of the immune system in a wide range of diseases (Panda et al. 2021; Tomasoni et al. 2013; Bruno et al. 2009; Lai et al. 2010; Yu et al. 2013; Feng et al. 2014; Wang et al. 2017; Xin et al. 2013a2013, 2013b; Doeppner et al. 2015).

Standing these points, sEVs hold great promise as therapeutics per se and as carrier systems for various drug delivery applications. However, one of the major challenges associated with their application is the efficient loading of drugs and time-consuming isolation methods (Park et al. 2019). To date, co-incubation, electroporation, saponin treatment, sonication, and extrusion are some of the most used methods for encapsulating active compounds (Nasiri Kenari, Cheng, and Hill 2020) and further methodologies are under investigation to enhance secretion (Hao et al. 2023). However, the advantages and drawbacks of each approach rely on the experimental settings, types of drugs, and source of sEVs (Romano, Netti, and Torino 2020; Wei et al. 2019; Fu et al. 2020; Gomari et al. 2019; Kooijmans et al. 2013; Vader et al. 2016; Podolak, Galanty, and Sobolewska 2010; Thakur et al. 2020).

In this study, we conducted a comparative analysis of the delivery efficacy of MSC-EVs encapsulated with doxorubicin (DXR-MSC-EVs) in both 2D and 3D CHS models. To achieve proper drug loading, we employed a novel and highly efficient encapsulation method based on high-pressure homogenization (HPH). Our previous research demonstrated the effectiveness of HPH in encapsulating the anticancer drug Irinotecan HCl Trihydrate into glioma cell (U87-MG)-derived sEVs, showing superior results compared to conventional incubation at 37°C for 2 h (hrs) (Romano, Netti, and Torino 2021). Here, we aimed to verify the reliability of HPH encapsulation method on EVs by evaluating a different cell line and anticancer drug. Following the characterization of physicochemical properties of DXR-MSC-EVs, we assessed their morphological integrity using transmission electron microscopy (TEM) and evaluated their uptake and cytotoxicity effects on SW1353 CHS cells grown models.

The conventional method for screening oncology drugs often involves utilizing 2D cell cultures. However, this approach may not always accurately predict the cytotoxic activity of drugs, a limitation that extends to sEVs. In contrast, 3D culturing preserves a composition heterogeneity akin to tumor tissue, mirroring the in vivo complexity, and offers additional advantages over conventional monolayered cell cultures, including retention of topology and meaningful cell-to-matrix interactions (Bordanaba-Florit et al. 2021).

To our knowledge, no study on sEVs for CHS using 3D culture has yet been conducted. Nevertheless, 3D cultures, like spheroids, better mimic the oxygen and pH gradients and the necrotic core of the tumor in vivo. These microenvironmental features significantly reduce the efficacy of standard chemotherapy, as we recently demonstrated for DXR and Cisplatin using SW1353 cells (Perut et al. 2018). So, here we evaluated the nano-biointeraction of DXR-MSC-EVs with such a complex environment through 2D and 3D testing.

2 | Materials and Methods

The mouse bone marrow MSC and Chondrosarcoma SW1353 cell lines were from the American Type Culture Collection (ATCC). Media, cell culture reagents and all other chemicals reagent grade were purchased from Sigma Aldrich (St. Louis, Missouri, USA). Doxorubicin HCl was from Selleckchem (Houston, USA).

2.1 | Cell Culture

To generate 3D spheroids, SW1353 cell line was seeded in 96-well Round Bottom Ultra-low attachment plates (Costar) at a density of $5*10^3$ cells/well and cultured in filtered IMDM (Iscove's Modified Dulbecco's Medium) supplemented with 10% fetal bovine serum (FBS). The plate was inverted, and cells were left to adhere overnight in an incubator with a gentle stirring at 37°C, a humidified atmosphere, containing 5% CO_2 and 95% air. After 24 h the plates were flipped again, 200 μL of medium were aspirated, and the formed spheroids were allowed to continue growing. Their growth was constantly monitored using a Nikon Eclipse-TE 2000-S microscope (Nikon, Tokyo, Japan).

10970290, 0, Downloaded from https://analyticalsciencejournals.onlinelibrary.wiley.com/doi/10.1002/bit.28969 by Enza Torino - Uni Federico II Di Napoli , Wiley Online Library on [19/12/2024]. See the Terms and Conditions (https://onlinelibrary.wiley.com/terms-and-conditions) on Wiley Online Library for rules of use; OA articles are governed by the applicable Creative Commons License

2.2 | sEVs Isolation

sEVs were isolated by sequentially centrifuge from the supernatant of MSCs culture media. Briefly, $4*10^6$ cells were seeded in a T150 flask and cultured to become 75% confluent. Then the supernatant was displaced with fresh DMEM without FBS for 48 h. The conditioned medium (CM) was collected, and sequentially centrifuged at $300 \times g$ for 10 min, $2000 \times g$ for 10 min and another 30 min at $10{,}000 \times g$ to dislodge cells and debris. sEVs were purified by dUC of supernatant using an OptimaTM MAX-XP Ultracentrifuge (Beckman Coulter, Brea, CA, USA) at ~110,000 $\times g$ (70,000 rpm – MLA-80 ROTOR) for 70 min. The sEVs isolated were pelleted in PBS and purified from protein aggregates with a second dUC wash at $110{,}000 \times g$ for 70 min. All procedures were carried out at 4°C. The purified sEVs were resuspended in 200 μL of PBS and stored at −20°C before use.

2.3 | Loading Capability of Therapeutic Cargo in MSC-EVs by HPH

To encapsulate sEVs with DXR, an HPH treatment was performed. In more detail, we investigated the encapsulation efficiency (EE) by the application of this novel technique testing three different concentrations of DXR (10.3–20.6–41.3 μM) premixed with a fixed concentration ($11.61*10^8$ particles/mL) of naïve sEVs in PBS. The samples were forced through a stainless-steel feed reservoir and subjected to a fixed Pressure set at 1500 bar for two cycles as previously reported (Romano, Netti, and Torino 2021). The collected samples were purified by a Spin-X corning Ultrafiltration System with a 3KDa Cut-off centrifuged at $3000 \times g$ up to 1 hr at 4°C. The final amount of encapsulated DXR was determined by UV-Vis Spectrophotometric analysis (330/110 nm-Mettler Toledo, USA) through a calibration curve at 480 nm.

2.4 | MSC-EVs Characterization: Size, Morphology, and Total Protein Analysis

After purification of naïve sEVs and engineering with DXR (DXR-MSC-EVs), Dynamic Light Scattering (DLS) was used to determine the hydrodynamic diameter of particles. Each sample was diluted 1:5 with 1 mL of PBS in a polystyrene 12-mm square glass cuvette (square aperture for 90° sizing Malvern; # PCS1115) and measured in triplicate at 25°C using a Zetasizer Nano ZS (Model ZEN3600, Malvern Instruments Ltd. UK) equipped with a solid-state laser ($\lambda = 633$ nm) at a scattering angle of 173°. Surface charge values were also obtained from zeta potential measurements of samples diluted 1:5 mL and performed at 25°C on a Zetasizer Nano ZS (Malvern Panalytical, UK) in triplicates, where each consisted of a minimum of ten individual runs. To capture CRYO-TEM micrographs, 3 μL of samples were directly dropped onto Formvar/Carbon 200 mesh Cu Agar grids. sEVs were observed in a Tecnai FEI TEM operated at 80 kV accelerating voltage. For each vesicle preparation, surface protein content was quantified with QuantiProTM BCA Assay Kit (Sigma Aldrich; St. Louis, Missouri, USA).

2.5 | EV-DXR Flow Cytometry Analysis

All flow cytometry experiments were conducted on BD FACSMelody^{TM}. Briefly, SW1353 cells were seeded in 48-well plates (Falcon) at a density of $1*10^5$ SW1353 cells/well and cultured in IMDM supplemented with 10% FBS and left to adhere for 24 h in an incubator with a humidified atmosphere, containing 5% CO_2 and 95% air. Afterward, cultured medium was replaced with the fresh one without FBS, supplemented with Free-DXR or DXR-MSC-EVs at the two fixed concentrations of 500 and 250 nM. The negative control consisted of cultured medium without FBS where the Free-DXR or DXR-MSC-EVs aliquots were replaced with an equal amount of PBS. Cells were incubated 72 hrs, rinsed three times with PBS (1×) to ensure particle removal from the outer cell membrane, removed by trypsinization and resuspended in cultured medium. The final samples were transferred into polystyrene round-bottomed tubes (Falcon), put on ice, and immediately analyzed by flow cytometry. A minimum of 10,000 events between three independent replicas were acquired per sample.

Forward scattering (FSC), side scattering (SSC), and fluorescence intensity mean (FI) parameters were analyzed to gain as much as possible information on the occurred internalization phenomena.

2.6 | In Vitro Cytotoxicity of DXR-MSC-EVs

The cells metabolic activity in the presence of DXR-MSC-EVs was analyzed up to 72 h using MTT assay on SW1353 and HEK293T cell monolayers. Briefly, $15*10^3$ SW1353 cells/well and $5*10^3$ HEK293T cells/well were seeded in 96-well plates with 200 μL of medium each and incubated overnight at 37°C and 5% CO_2. Survival rates for DXR-MSC-EVs treated cells were compared to Free-DXR treated cells in a range between 1 and 250 nM up to 72 h of incubation. MTT was added to each well and incubated at 37°C for additional 3 h. Supernatants were completely removed, and the purple formazan crystals produced were dissolved in 100 μL of dimethyl sulfoxide (DMSO). Absorbance was determined at 545–630 nm using a spectrophotometer microplate reader. All experiments were repeated threetimes and results were expressed as the viable cells percentage with respect to the control.

The cell viability on 3D model was investigated by the acid phosphatase assay (APC) after 1 week from spheroid formation. In more detail, we selected 250–500 nM as the two lowest efficient concentrations of Free-DXR and DXR-MSC-EVs for cells testing. After 48 h of incubation, cells were rinsed with 200 μL/well of PBS, and 100 μL/well of NaAc-buffer (Sodium Acetate, Sigma–Aldrich, Milan, Italy) containing p-Nitrophenyl phosphate disodium hexahydrate. After 2 h of incubation at 37°C and 5% CO_2, NaOH 1 M (10 μL/well) was added to stop the reaction. A microplate reader (Tecan Infinite F200pro, Tecan, Milan, Italy) was used to record the absorbance at 405 nm. Results were expressed as the viable cells percentage with respect to the control.

10970290, 0, Downloaded from https://analyticalsciencejournals.onlinelibrary.wiley.com/doi/10.1002/bit.28909 by Enza Torino - Uni Federico II Di Napoli , Wiley Online Library on [19/12/2024]. See the Terms and Conditions (https://onlinelibrary.wiley.com/terms-and-conditions) on Wiley Online Library for rules of use; OA articles are governed by the applicable Creative Commons License

2.7 | Up-Take Assay in 3D Spheroids by Dual-Photon Confocal Microscopy

3D spheroids were obtained as described above. At 7 days of culture, spheroids were then treated with DXR or DXR-MSC-EVs at a final concentration of 500 nM. After 24 h cells were incubated for 30 min with Hoechst 33258 (20 μg/mL) and observed at the confocal microscope. Confocal images were collected by using A1R MP multiphoton confocal microscope (GaAsP) and NIS-Element AR software (Nikon). We used a manual optical path mode and a custom channel series mode, with first dichroic mirror total reflection for IR, a first filter cube 492 SP, and a second filter cube 525/50, and a third filter cube 575/25, laser wavelength 800, laser power 29.3, for R-CH1 PMT HV 43, PMT Offset -62; for R-CH2 PMT HV 45, PMT Offset-102. Objective 25× (water) with a numerical aperture 1.1, refraction index 1.333, Resonant scanning.

2.8 | Statistics

Statistical analysis was performed using the GraphPad Prism 7 software for Windows. Results were reported as Mean ± Standard Error (SD) and the differences were analyzed using non-parametric Mann–Whitney test for the difference between groups. Only $p < 0.05$ were considered significant.

3 | Results

3.1 | MSC-EVs Stability After DXR Entrapment With HPH System

Herein, the effectiveness of HPH treatment for an efficient entrapment of DXR in MSC-EVs was investigated at three different theoretical concentrations of DXR (10.3, 20.6 and 41.3 μM respectively) considering the ideal dosages range stated in previous works (Wei et al. 2019; Goh et al. 2017; Tian et al. 2014) (Figure 1).

Notably, a final EE over 30% was reached regardless of the initial amount of Free-drug mixed with naïve vesicles, in line with our previous findings on tumoral glioblastoma-U87 derived sEVs encapsulating Irinotecan (Romano, Netti, and Torino 2021). These results confirmed that HPH for drug loading can also be applied to several types of nanovesicles to obtain a temporary deformation, such as in the case of MSC-derived EVs with a different proteolipid structure, as reported by Haraszti et al. 2016 with respect to U87 derived sEVs.

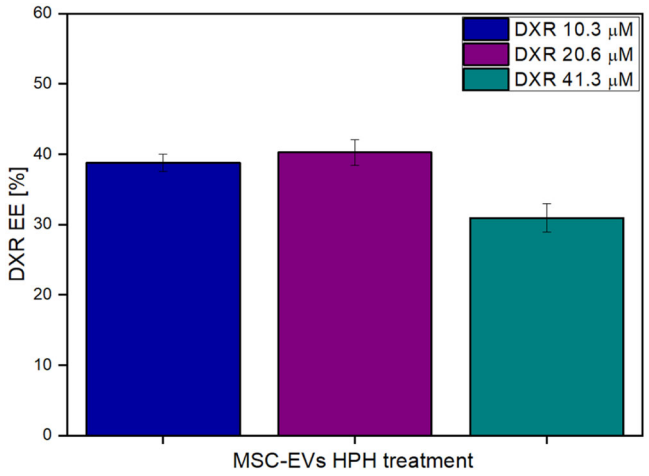

FIGURE 1 | EE% of DXR into sEVs at three fixed concentration (10.3, 20.6 and 41.3 μM) by HPH treatment.

To assess the morphological integrity of sEVs after HPH treatment, CRYO-TEM analysis was performed. In more detail, Figure 2a shows that the typical sEVs structure was preserved after DXR entrapment in the lipidic bilayer. Figure 2b reports the sEVs average size change before and after the HPH treatment. Notably, naïve empty MSC-sEVs present a narrow size distribution with a peak diameter of 159 nm while a slight increase (167 nm) is visible in DXR-MSC-sEVs loaded with the highest DXR concentration (41.3 μM).

To further assess the effect of HPH on the sEVs bilayer stability, Zeta Potential, and the surface protein content analysis (Figure 2c,d, respectively) were reported. Stable values comparing empty MSC-EVs and DXR-MSC-EVs at higher theoretical concentrations revealed that both the surface charge and the total protein amount remained nearly unchanged after HPH treatment. This finding suggests that the encapsulation did not affect sEVs stability.

3.2 | Preliminary in Vitro Investigation of DXR-MSC-EVs Cytotoxic Activity and Internalization Phenomena in a CHS 2D Model

The cytotoxic effect of DXR-MSC-EVs in tumoral microenvironment was preliminary tested in vitro on SW1353 cells incubated with PBS (control), DXR, or DXR-MSC-EVs respectively, up to 72 h.

By comparing Free-DXR and DXR-MSC-EVs we evaluated whether MSC-EVs used as drug delivery systems could favor drug uptake and activity. Furthermore, we explored a wide range of DXR dosages, between 1 and 250 nM at 24, 48 and 72 h, to include different IC50 values described in the literature for SW1353 cells treated with DXR (Perut et al. 2018; Monderer et al. 2013; Palubeckaitė et al. 2020) (Figure 3a). Interestingly, we found that DXR-MSC-EVs treatment was much more effective in inhibiting cell proliferation than Free-DXR treatment at the same concentration. According to previously published data (Perut et al. 2018), Free-DXR reduced cell viability by 50% at 66 nM concentration at 72 h, while DXR-MSC-EVs treatment significantly decreased cell viability at lower doses (Figure 3a,b).

The tumor-targeting capability of MSCs was further emphasized by the selective cytotoxic effect of DXR-MSC-EVs on cancer cells compared to healthy HEK293T cells. While SW1353 cells were highly responsive to DXR-MSC-EVs, the noncancerous cell line HEK293T showed much less sensitivity (Supporting Information S1: Figure S1a,b).

Consistent with previous studies (Mehdizadeh, Ataei, and Hosseinkhani 2020; Łażewska et al. 2020; Benyettou et al. 2017),

10970290, 0, Downloaded from https://analyticalsciencejournals.onlinelibrary.wiley.com/doi/10.1002/bit.28969 by Enza Torino - Uni Federico II Di Napoli , Wiley Online Library on [19/12/2024]. See the Terms and Conditions (https://onlinelibrary.wiley.com/terms-and-conditions) on Wiley Online Library for rules of use; OA articles are governed by the applicable Creative Commons License

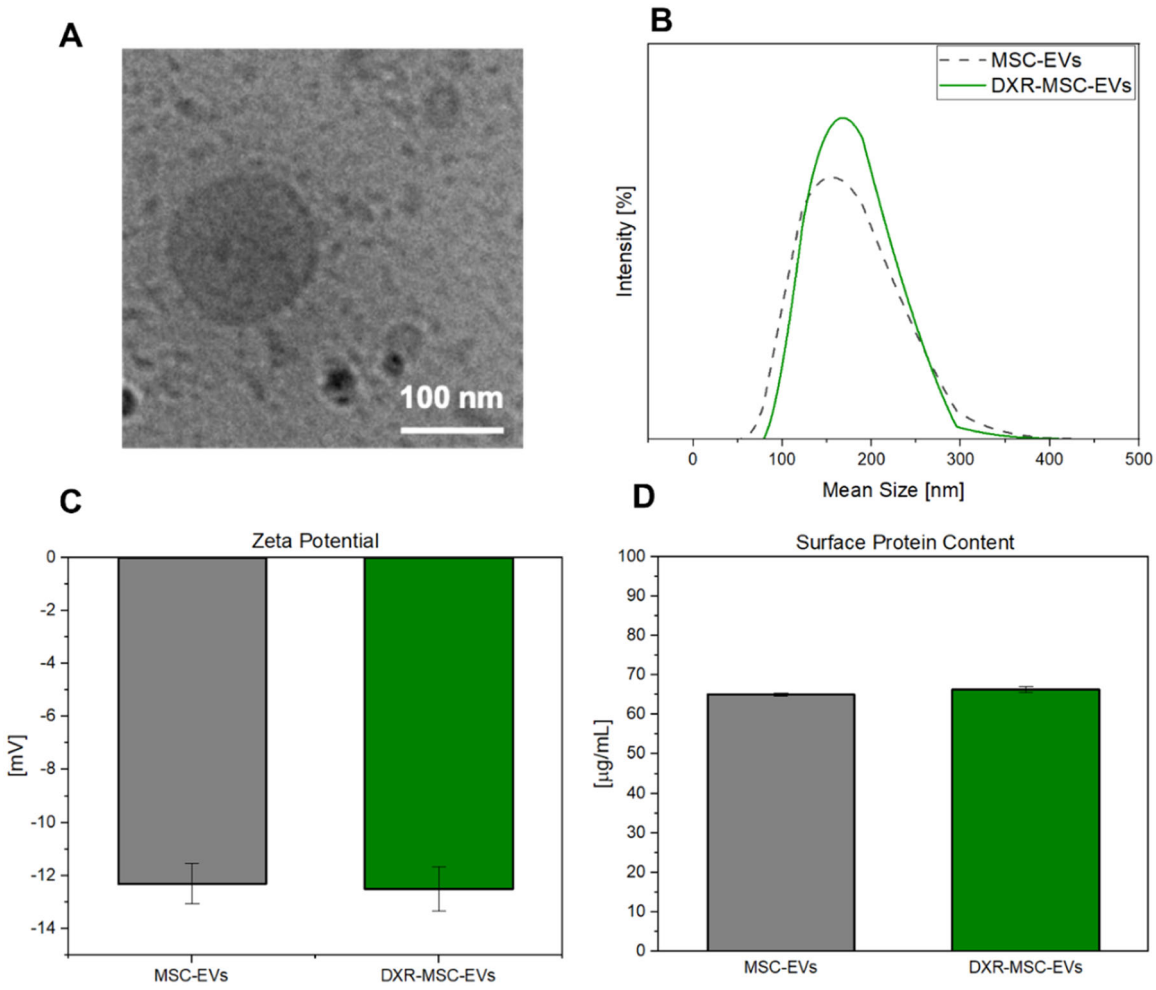

FIGURE 2 | Comparison between MSC-EVs and DXR-MSC-EVs at 41.3 µM by HPH at 1500 bar-two cycles: (a) CRYO-TEM observation; (b) Particle size distribution by DLS, (c) Zeta potential, (d) Total protein amount by BCA assay.

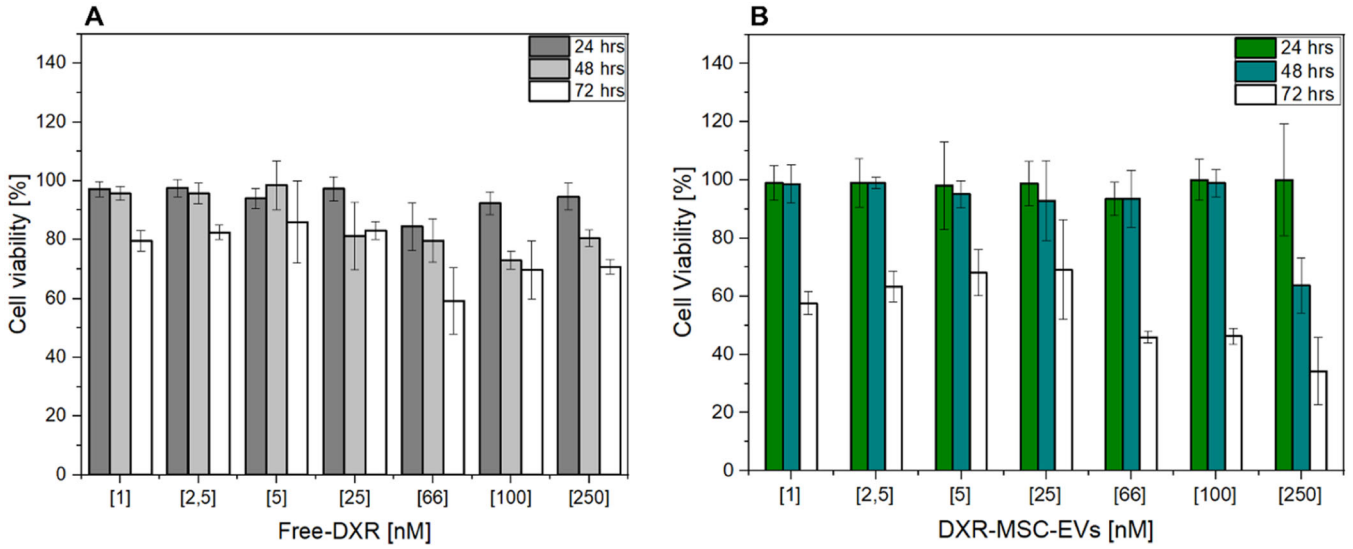

FIGURE 3 | In vitro cytotoxicity of Free-DXR and DXR-MSC-EVs, SW1353 cells exposure to (a) Free-DXR and DXR-MSC-EVs (b) activity in the range 1–250 nM within 72 h. All data are presented as mean ± SD ($n = 3$).

10970290, 0, Downloaded from https://analyticalsciencejournals.onlinelibrary.wiley.com/doi/10.1002/bit.28969 by Enza Torino - Uni Federico II Di Napoli , Wiley Online Library on [19/12/2024]. See the Terms and Conditions (https://onlinelibrary.wiley.com/terms-and-conditions) on Wiley Online Library for rules of use; OA articles are governed by the applicable Creative Commons License

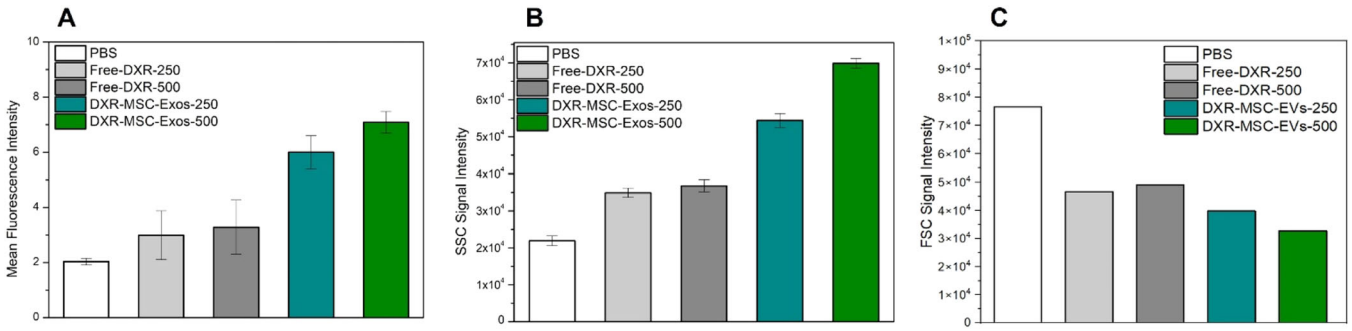

FIGURE 4 | DXR-MSC-EVs and Free-DXR internalization with SW1353 cells quantified by flow cytometry measurements at 72 hrs of treatment: (a) FI, (b) SSC signal, (c) FSC signal. All data are presented as mean ± SD ($n = 3$).

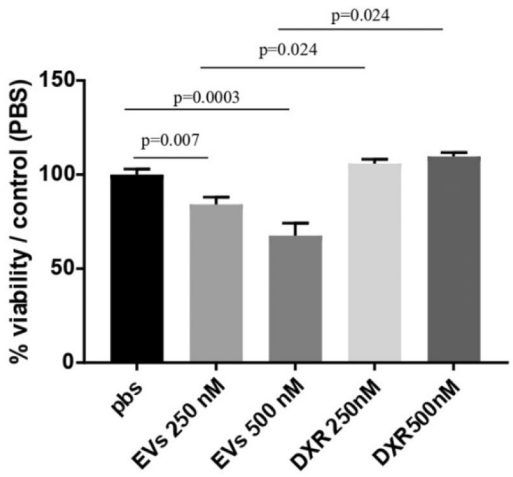

FIGURE 5 | SW1353 hanging drop spheroid. % cell viability upon Free-DXR and DXR-MSC-EVs treatment on CHS 3D cultures. Differences between spheroids groups were analyzed with Mann–Whitney U test.

HEK293T cells exhibited high sensitivity to Free-DXR with significant cytotoxicity and reduced cell viability (almost to 55% at a concentration of 66 nM after 48 h) (Supporting Information S1: Figure S1a). In contrast, DXR-MSC-EVs led to only moderate cytotoxicity in HEK293T cells, with a 49% reduction in cell viability at the much higher concentration of 250 nM only after 72 h (Supporting Information S1: Figure S1b).

Notably, SW1353 cells displayed enhanced sensitivity to DXR-MSC-EVs (Figure 3b), suggesting that MSC-EVs can effectively bypass drug resistance mechanisms seen in this cell line (Hsieh et al. 2020). This highlights MSCs' unique capability to home in on tumor-associated stroma, positioning them as promising delivery vehicles for targeting and releasing therapeutic drugs directly within the tumor microenvironment.

Once identified the highest cytotoxic effects in term of DXR dosage and time-exposures, we further investigated DXR-MSC-EVs nano-biointeraction at the interface of tumoral cells by flow cytometry quantitative measurements (Figure 4a–c). Two DXR concentrations (250 and 500 nM) were selected and tested both in a Free-drug solution and the sEVs nanodelivery system. Figure 4a reports the FI as an indirect parameter of the internalization phenomena occurred upon the 72 h cells treatment. Notably, DXR-MSC-EVs-500 (with a DXR dosage of 500 nM) reached the highest internalization value compared to Free-DXR, resulting in a more selective and efficient targeting at nanoscale. A progressive increase in cell granularity revealed by SSC signals (Figure 4b), may be associated with increased uptake of DXR, as observed in melanoma cells model by using synthetic nanoparticles loaded with DXR (Toderascu et al. 2023).

To further corroborate our hypothesis, the FSC measurement was investigated as a cell viability indicator, to assess the therapeutic potential of DXR-MSC-EVs (Figure 4c) compared to the Free-drug. Indeed, FSC intensity is proportional to the size of cells. As reported by others (Tammaro et al. 2020; Jochums et al. 2017; Ha, Chung, and Yoon 2020), a reduction in FSC intensity can reflect cell shrinkage and may also provide indirect information about the toxicity of the treatment. In line with cytotoxicity analysis, the FSC value was lower for DXR-MSC-EVs in a dose-dependent manner than for Free-DXR. Variation of Standard Deviation is very low and not appreciable in the graphs reported in Figure 4c.

3.3 | DXR-MSC-EVs Are an Effective Drug Delivery System to Inhibit the Growth of 3D-Cultures of CHS

Once SW1353 spheroids were completely formed and reached a diameter of approximately 500 μm, a 48 h treatment with either free or encapsulated DXR was conducted to test the cell viability. In line with previous studies (Perut et al. 2018), a selective chemoresistance of 3D-CHS model treated with Free-DXR was confirmed. Notably, we observed a significant dose-dependent inhibition of cell growth with DXR carried by MSC-EVs (Figure 5).

We then evaluated the uptake at 24 h of DXR from CHS spheroids, treated with DXR-MSC-EVs or Free-DXR, at the dual-photon confocal microscope. Spheroids showed a diameter of around 300–500 μm. We confirmed that DXR was uptaken from CHS cells in both conditions, although in cells treated with Free-DXR, the intracellular fluorescent signals of DXR appeared to be higher and more diffuse in the spheroids (Figure 6a). However, in DXR-MSC-EVs treated spheroids, the total number of cells/spheroid appeared to be lower, and nuclei were more fragmented than in the Free-drug-treated spheroids,

10970290, 0, Downloaded from https://analyticalsciencejournals.onlinelibrary.wiley.com/doi/10.1002/bit.28969 by Enza Torino - Uni Federico II Di Napoli , Wiley Online Library on [19/12/2024]. See the Terms and Conditions (https://onlinelibrary.wiley.com/terms-and-conditions) on Wiley Online Library for rules of use; OA articles are governed by the applicable Creative Commons License

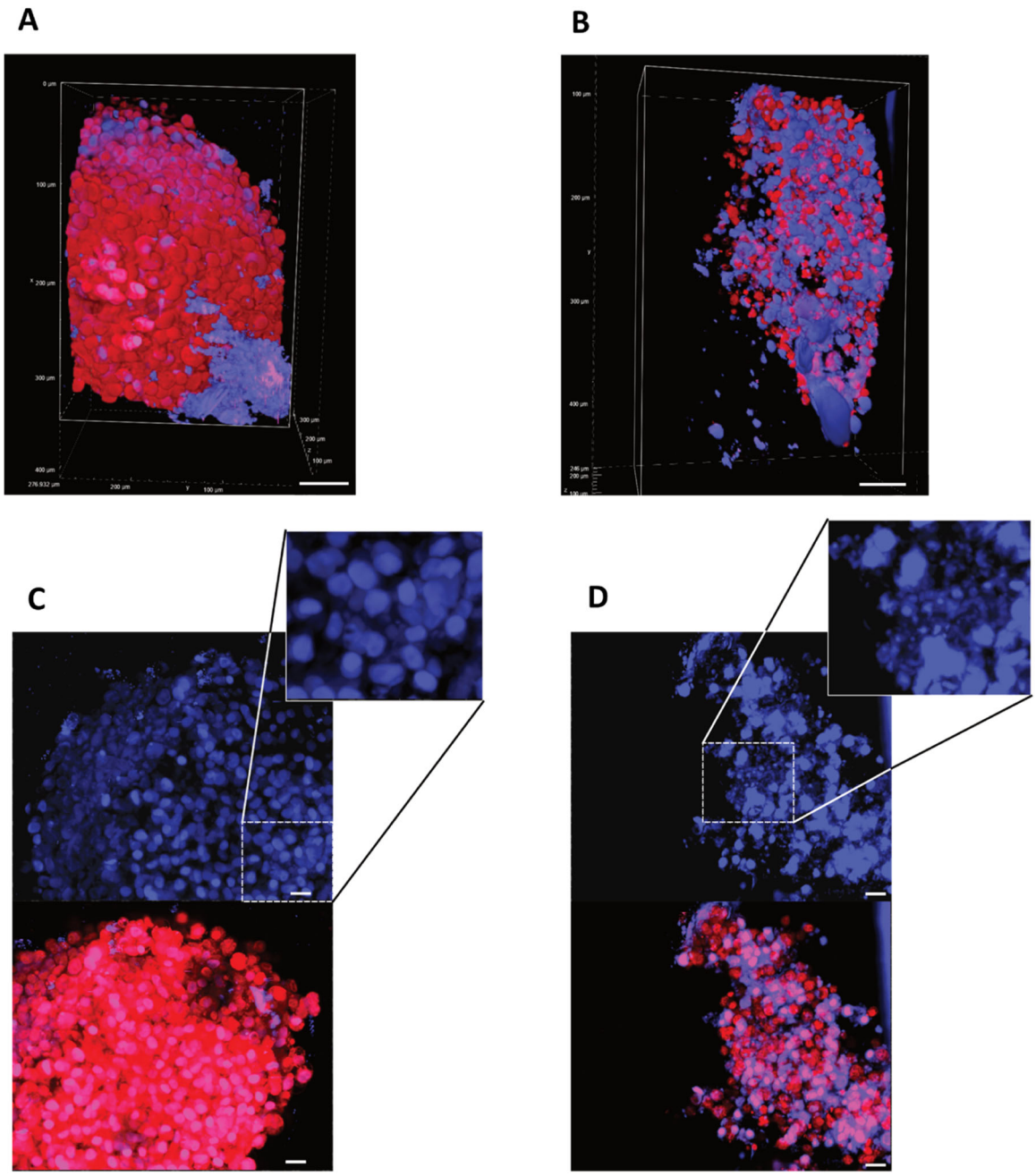

FIGURE 6 | Dual photon confocal analysis of live CHS SW1353 spheroids, treated with (a) Free-DXR or with (b) DXR-MSC-EVs. DXR uptake was visualized by the red autofluorescent signal of DXR. Nuclei were counterstained with Hoechst 33258. For DXR, 108 z-step (3 μm deep); for DXR-MSC-EVs, 82 z-step (3 μm deep). For both samples, we used immersion objective 25× (water), line average 8, pinhole size 255.4 μm, scan speed 7.5, zoom 1.0. Volume render (blending alpha) of one representative spheroid for each condition is reported with a scale bar 50 μm.Maximum Intensity projection of (c) Free-DXR and (d) DXR-MSC-EVs. Scale bar 20 μm. A higher magnification is represented in the squares.

suggesting the presence of a higher number of necrotic cells and a more toxic effect due to DXR-MSC-EVs (Figure 6b).

4 | Discussion and Conclusions

sEVs are nano-sized, lipid membrane–enclosed vesicles secreted by nearly all cell types. These cell-derived membranous particles are highly enriched in lipids, proteins, and various nucleic acids, and play a pivotal role as mediators of intercellular communication in various physiopathological conditions. Their remarkable ability to transfer bioactive components and navigate biological barriers has spurred an escalating exploration of sEVs as potential delivery vehicles. Our recent work (Costagliola di Polidoro et al. 2023) also compared sEVs' role in triggering pharmacodynamics with respect to polymer nanoparticles, highlighting the urgent need for an optimal design of drug delivery systems.

Given their potential innate advantages, different drug-loading methods in sEVs have been investigated (Fu et al. 2020). However, sEVs-based drug delivery remains challenging due to the

10970290, 0, Downloaded from https://analyticalsciencejournals.onlinelibrary.wiley.com/doi/10.1002/bit.28909 by Erica Torino - Uni Federico II Di Napoli , Wiley Online Library on [19/12/2024]. See the Terms and Conditions (https://onlinelibrary.wiley.com/terms-and-conditions) on Wiley Online Library for rules of use; OA articles are governed by the applicable Creative Commons License

poor drug loading efficiency, time-consuming procedures that can compromise sEVs integrity, and a lack of industrial scale-up methodology for clinical translation (Keysberg et al. 2023; Zhang et al. 2024). To tackle these challenges, our prior research introduced High-Pressure Homogenization as an innovative approach to enhance drug encapsulation in sEVs (Romano, Netti, and Torino 2021). This one-step pharmaceutical process stands out from traditional techniques, as it is scalable and enables high throughput encapsulation of anticancer drugs without affecting sEVs morphology and functionality.

The objective of our study was to validate the efficacy of our innovative encapsulation method utilizing High-Pressure Homogenization for entrapping active compounds in sEVs sourced from MSC. It's noteworthy that mouse MSC-EVs exhibit a distinct external lipidic profile, characterized by a significant enrichment in fatty acid that are typically depleted in tumoral sEVs, such as U87-MG sEVs (Haraszti et al. 2016). Moreover, their profile includes leukotrienes, arachidonic acid (AA), phosphatidic acid, prostaglandins Lys-phosphatidylcholine (LPC), and docosahexaenoic acid (DHA) (Skotland et al. 2020).

In our novel approach employing dynamic High-Pressure Homogenization (Romano, Netti, and Torino 2021), we subject the lipidic bilayer to physical stress, inducing a transient manipulation. Our hypothesis posits that this manipulation primarily involves lipids inhigher percentages, such as cholesterol and phosphatidylserine, which are prevalent in most sEVs. Importantly, this process does not compromise the morphological integrity or biological identity of sEVs. Here, applying this principle, we successfully encapsulated the chemotherapeutic drug doxorubicin (DXR) in MSC-derived EVs, achieving an encapsulation efficiency exceeding 40%. Notably, this outcome aligns with our earlier findings with the chemotherapeutic agent irinotecan. Additionally, consistent with previous reports, we demonstrated effective control over the surface fluidity of the lipidic bilayer in various sEVs, irrespective of their composition. This ensures minimal interference from minor lipid components that could impact membrane fluidity.

Once we obtained the engineered DXR-MSC-EVs, we evaluated their potential role as drug carriers in CHS treatment, testing their internalization and cytotoxicity effect in both 2D and 3D SW1315 cell models. Currently, chemoresistance is a major issue for the successful treatment of CHS, and there is still an urgent and unmet need to assess the effectiveness of therapeutic agents trough predictable and reliable preclinical models. In this scenario, 3D cell culture perfectly mirrors the physiopathology conditions of such a complex microenvironment as the CHS tumor, better than traditional monolayer cultures. For instance, in a recent publication (Perut et al. 2018) the limited efficacy of conventional anticancer drugs was confirmed trough the in vitro testing on CHS 3D models. The reason for this is that drug resistance in 3D-CHS cultures derives from the peculiar microenvironmental feature of 3D cell growing structure over traditional 2D cultures: the proliferation rate, degree of differentiation, level of cell-to-cell interaction and cell-to-matrix as well as drug diffusion and drug resistance (Lv et al. 2017; Weigelt, Ghajar, and Bissell 2014) are just some of the main key aspects to consider. Furthermore, 3D organoid-like cultures rely on cell autonomy or cell–cell interactions and intrinsic or extrinsic biochemical signals that constitute the tumor microenvironment, including local hypoxia, low access to nutrients, acidosis, and chemical and physical barriers to the perfusion of drugs. Establishing low pH and decreased oxygen tension conditions are particularly important for CHS, as these tumors are not vascularized and are highly hypoxic tumors (Bovée et al. 2010), and both these features can greatly reduce drug efficacy.

To our knowledge, this study marks the pioneering demonstration of the efficacy of MSC-EVs loaded with the chemotherapeutic drug DXR as a potent nanodrug, validated in both 2D and 3D CHS models (Wei et al. 2019, 2022). Indeed, we obtained DXR-MSC-EVs with a very high encapsulation efficiency if compared to DXR entrapped in an analog mouse MSC-EVs model with a different technique (Wei et al. 2019). Moreover, DXR-MSC-EVs could be taken up by SW1315 cells and induce cytotoxicity. The study on 2D model revealed higher toxicity of DXR-MSC-EVs, compared with Free-DXR, probably due to higher uptake. Intriguingly, the cytotoxic effect of DXR-MSC-EVs was exclusively evident in the more pharmacologically relevant 3D model, demonstrating a dose-dependent response. We employed dual-photon microscopy to confirm the presence of DXR within the spheroid, revealing numerous cells with fragmented nuclei, indicating a higher prevalence of necrotic cells in the spheroid treated with DXR encapsulated in EVs compared to Free-DXR.

5 | Conclusions

In conclusion, sEVs hold significant promise in disease management. Our results underscored the potential of HPH treatment as a novel and efficient system for the rapid and scalable encapsulation of sEVs with various compounds. Additionally, our studies demonstrated the remarkable effectiveness of the engineered DXR-MSC-EVs in penetrating a 3D model of CHS compared to Free-DXR. This observation highlights the notion that the delivery dynamics of sEVs can instigate, unique set of nano-biointeractions, ultimately influencing their fate in both the extracellular and intracellular compartments.

Author Contributions

Eugenia Romano: conceptualization, data curation, formal analysis, investigation, methodology, paper writing (original draft and review and editing), visualization. **Francesca Perut:** data curation, formal analysis, investigation, methodology and paper writing. **Sofia Avnet:** data curation, formal analysis, investigation, methodology and paper writing. **Gemma Di Pompo:** data curation, formal analysis, investigation, methodology. **Simona Silvestri:** formal analysis. **Felicia Roffo:** formal analysis. **Nicola Baldini:** visualization. **Paolo Antonio Netti:** visualization. **Enza Torino:** conceptualization, data curation, formal analysis, investigation, methodology, paper writing (original draft and review and editing), visualization, funding acquisition, supervision.

Acknowledgments

The authors have nothing to report. Open access publishing facilitated by Universita degli Studi di Napoli Federico II, as part of the Wiley - CRUI-CARE agreement.

10970290, 0, Downloaded from https://analyticalsciencejournals.onlinelibrary.wiley.com/doi/10.1002/bit.28969 by Enza Torino - Uni Federico II Di Napoli , Wiley Online Library on [19/12/2024]. See the Terms and Conditions (https://onlinelibrary.wiley.com/terms-and-conditions) on Wiley Online Library for rules of use; OA articles are governed by the applicable Creative Commons License

Conflicts of Interest

The authors declare no conflicts of interest.

Data Availability Statement

The data that support the findings of this study are available from the corresponding author upon reasonable request.

References

Benyettou, F., H. Fahs, R. Elkharrag, et al. 2017. "Selective Growth Inhibition of Cancer Cells With Doxorubicin-Loaded Cb [7]-Modified Iron-Oxide Nanoparticles." *RSC Advances* 7, no. 38: 23827–23834.

Bordanaba-Florit, G., I. Madarieta, B. Olalde, J. M. Falcón-Pérez, and F. Royo. 2021. "3D Cell Cultures as Prospective Models to Study Extracellular Vesicles in Cancer." *Cancers* 13, no. 2: 307.

Bovée, J. V. M. G., P. C. W. Hogendoorn, J. S. Wunder, and B. A. Alman. 2010. "Cartilage Tumours and Bone Development: Molecular Pathology and Possible Therapeutic Targets." *Nature Reviews Cancer* 10, no. 7: 481–488.

Bruno, S., C. Grange, M. C. Deregibus, et al. 2009. "Mesenchymal Stem Cell-Derived Microvesicles Protect Against Acute Tubular Injury." *Journal of the American Society of Nephrology* 20, no. 5: 1053–1067.

Chongchai, A., K. Bentayebi, G. Chu, et al. 2024. "Targeted Treatment of Chondrosarcoma With a Bacteriophage-Based Particle Delivering a Secreted Tumor Necrosis Factor-Related Apoptosis-Inducing Ligand." *Molecular Therapy Oncology* 32, no. 2: 200805. https://doi.org/10.1016/j.omton.2024.200805.

Costagliola di Polidoro, A., Z. Baghbantarghdari, V. De Gregorio, S. Silvestri, P. A. Netti, and E. Torino. 2023. "Insulin Activation Mediated by Uptake Mechanisms: A Comparison of the Behavior Between Polymer Nanoparticles and Extracellular Vesicles in 3D Liver Tissues." *Biomacromolecules* 24, no. 5: 2203–2212.

Doeppner, T. R., J. Herz, A. Görgens, et al. 2015. "Extracellular Vesicles Improve Post-Stroke Neuroregeneration and Prevent Postischemic Immunosuppression." *Stem Cells Translational Medicine* 4, no. 10: 1131–1143.

Donati, D. M., and G. Bianchi. 2020. *Chondrosarcomas (CHS). Diagnosis of Musculoskeletal Tumors and Tumor-like Conditions*. Springer, 157–179.

Elliott, R. O., and M. He. 2021. "Unlocking the Power of Exosomes for Crossing Biological Barriers in Drug Delivery." *Pharmaceutics* 13, no. 1: 122.

Feng, Y., W. Huang, M. Wani, X. Yu, and M. Ashraf. 2014. "Ischemic Preconditioning Potentiates the Protective Effect of Stem Cells Through Secretion of Exosomes by Targeting Mecp2 Via Mir-22." *PLoS One* 9, no. 2: e88685.

Fu, S., Y. Wang, X. Xia, and J. C. Zheng. 2020. "Exosome Engineering: Current Progress in Cargo Loading and Targeted Delivery." *NanoImpact* 20: 100261.

Goh, W. J., C. K. Lee, S. Zou, E. Woon, B. Czarny, and G. Pastorin. 2017. "Doxorubicin-Loaded Cell-Derived Nanovesicles: An Alternative Targeted Approach for Anti-Tumor Therapy." *International Journal of Nanomedicine* 12: 2759–2767.

Gomari, H., M. Forouzandeh Moghadam, M. Soleimani, M. Ghavami, and S. Khodashenas. 2019. "Targeted Delivery of Doxorubicin to HER2 Positive Tumor Models." *International Journal of Nanomedicine* 14: 5679–5690.

Guan, Y., W. Zhang, Y. Mao, et al. 2024. "Nanoparticles and Bone Microenvironment: A Comprehensive Review for Malignant Bone Tumor Diagnosis and Treatment." *Molecular Cancer* 23: 246. https://doi.org/10.1186/s12943-024-02161-1.

Ha, M. K., K. H. Chung, and T. H. Yoon. 2020. "Heterogeneity in Biodistribution and Cytotoxicity of Silver Nanoparticles in Pulmonary Adenocarcinoma Human Cells." *Nanomaterials* 10, no. 1: 36.

Hao, R., S. Hu, H. Zhang, et al. 2023. "Mechanical Stimulation on a Microfluidic Device to Highly Enhance Small Extracellular Vesicle Secretion of Mesenchymal Stem Cells." *Materials Today Bio* 18: 100527.

Haraszti, R. A., M.-C. Didiot, E. Sapp, et al. 2016. "High-Resolution Proteomic and Lipidomic Analysis of Exosomes and Microvesicles From Different Cell Sources." *Journal of Extracellular Vesicles* 5, no. 1: 32570.

Hsieh, M. J., C. Huang, C. C. Lin, et al. 2020. "Basic Fibroblast Growth Factor Promotes Doxorubicin Resistance in Chondrosarcoma Cells by Affecting XRCC5 Expression." *Molecular Carcinogenesis* 59, no. 3: 293–303.

Jafari, D., S. Shajari, R. Jafari, et al. 2020. "Designer Exosomes: A New Platform for Biotechnology Therapeutics." *BioDrugs* 34: 567–586.

Jochums, A., E. Friehs, F. Sambale, A. Lavrentieva, D. Bahnemann, and T. Scheper. 2017. "Revelation of Different Nanoparticle-Uptake Behavior in Two Standard Cell Lines NIH/3T3 and A549 by Flow Cytometry and Time-Lapse Imaging." *Toxics* 5, no. 3: 15.

Keysberg, C., O. Hertel, R. Hoffrogge, et al. 2023. "Hyperthermic Shift and Cell Engineering Increase Small Extracellular Vesicle Production in HEK293F Cells." *Biotechnology and Bioengineering* 121, no. 3: 942–958.

Kim, D. H., H. S. Lee, Y.-H. Mun, et al. 2020. "An Overview of Chondrosarcoma With a Focus on Nanoscale Therapeutics." *Journal of Pharmaceutical Investigation* 50: 537–552.

Kooijmans, S. A. A., S. Stremersch, K. Braeckmans, et al. 2013. "Electroporation-Induced siRNA Precipitation Obscures the Efficiency of siRNA Loading Into Extracellular Vesicles." *Journal of Controlled Release* 172, no. 1: 229–238.

Lai, R. C., F. Arslan, M. M. Lee, et al. 2010. "Exosome Secreted by MSC Reduces Myocardial Ischemia/Reperfusion Injury." *Stem Cell Research* 4, no. 3: 214–222.

Lv, D., Z. Hu, L. Lu, H. Lu, and X. Xu. 2017. "Three-Dimensional Cell Culture: A Powerful Tool in Tumor Research and Drug Discovery." *Oncology Letters* 14, no. 6: 6999–7010.

Łłażewska, D., A. Olejarz-Maciej, D. Reiner, et al. 2020. "Dual Target Ligands With 4-tert-butylphenoxy Scaffold as Histamine H3 Receptor Antagonists and Monoamine Oxidase B Inhibitors." *International Journal of Molecular Sciences* 21, no. 10: 3411.

Mehdizadeh, K., F. Ataei, and S. Hosseinkhani. 2020. "Effects of Doxorubicin and Docetaxel on Susceptibility to Apoptosis in High Expression Level of Survivin in HEK and HEK-S Cell Lines As in Vitro Models." *Biochemical and Biophysical Research Communications* 532, no. 1: 139–144.

Monderer, D., A. Luseau, A. Bellec, et al. 2013. "New Chondrosarcoma Cell Lines and Mouse Models to Study the Link Between Chondrogenesis and Chemoresistance." *Laboratory Investigation* 93, no. 10: 1100–1114.

Nasiri Kenari, A., L. Cheng, and A. F. Hill. 2020. "Methods for Loading Therapeutics Into Extracellular Vesicles and Generating Extracellular Vesicles Mimetic-Nanovesicles." *Methods* 177: 103–113.

Nazeri, E., M. Gouran Savadkoohi, K. Majidzadeh-A, and R. Esmaeili. 2018. "Chondrosarcoma: An Overview of Clinical Behavior, Molecular Mechanisms Mediated Drug Resistance and Potential Therapeutic Targets." *Critical Reviews in Oncology/Hematology* 131: 102–109.

Palubeckaitė, I., S. Venneker, I. H. Briaire-de Bruijn, et al. 2020. "Selection of Effective Therapies Using Three-Dimensional in Vitro Modeling of Chondrosarcoma." *Frontiers in Molecular Biosciences* 7: 566291.

Panda, B., Y. Sharma, S. Gupta, and S. Mohanty. 2021. "Mesenchymal Stem Cell-Derived Exosomes as an Emerging Paradigm for Regenerative Therapy and Nano-Medicine: A Comprehensive Review." *Life* 11, no. 8: 784.

Park, K.-S., E. Bandeira, G. V. Shelke, C. Lässer, and J. Lötvall. 2019. "Enhancement of Therapeutic Potential of Mesenchymal Stem Cell-

10970290, 0, Downloaded from https://analyticalsciencejournals.onlinelibrary.wiley.com/doi/10.1002/bit.28969 by Enza Torino - Uni Federico II Di Napoli , Wiley Online Library on [19/12/2024]. See the Terms and Conditions (https://onlinelibrary.wiley.com/terms-and-conditions) on Wiley Online Library for rules of use; OA articles are governed by the applicable Creative Commons License

Derived Extracellular Vesicles." *Stem Cell Research & Therapy* 10, no. 1: 288.

Perut, F., F. V. Sbrana, S. Avnet, A. De Milito, and N. Baldini. 2018. "Spheroid-Based 3D Cell Cultures Identify Salinomycin as a Promising Drug for the Treatment of Chondrosarcoma." *Journal of Orthopaedic Research* 36, no. 8: 2305–2312.

Pieretti, J. C., W. R. Rolim, F. F. Ferreira, C. B. Lombello, M. H. M. Nascimento, and A. B. Seabra. 2020. "Synthesis, Characterization, and Cytotoxicity of Fe3O4@ Ag Hybrid Nanoparticles: Promising Applications in Cancer Treatment." *Journal of Cluster Science* 31, no. 2: 535–547.

Podolak, I., A. Galanty, and D. Sobolewska. 2010. "Saponins as Cytotoxic Agents: A Review." *Phytochemistry Reviews* 9, no. 3: 425–474.

Romano, E., P. A. Netti, and E. Torino. 2020. "Exosomes in Gliomas: Biogenesis, Isolation, and Preliminary Applications in Nanomedicine." *Pharmaceuticals* 13, no. 10: 319.

Romano, E., P. A. Netti, and E. Torino. 2021. "A High Throughput Approach Based on Dynamic High Pressure for the Encapsulation of Active Compounds in Exosomes for Precision Medicine." *International Journal of Molecular Sciences* 22, no. 18: 9896.

Sha, B., W. Gao, Y. Han, et al. 2013. "Potential Application of Titanium Dioxide Nanoparticles in the Prevention of Osteosarcoma and Chondrosarcoma Recurrence." *Journal of Nanoscience and Nanotechnology* 13, no. 2: 1208–1211.

Shield, W. P., A. Cellini, H. Tian, et al. 2020. "Selective Agonists of Nuclear Retinoic Acid Receptor Gamma Inhibit Growth of HCS-2/8 Chondrosarcoma Cells." *Journal of Orthopaedic Research* 38, no. 5: 1045–1051.

Simard, F. A., I. Richert, A. Vandermoeten, et al. 2017. "Description of the Immune Microenvironment of Chondrosarcoma and Contribution to Progression." *Oncoimmunology* 6, no. 2: e1265716.

Skotland, T., K. Sagini, K. Sandvig, and A. Llorente. 2020. "An Emerging Focus on Lipids in Extracellular Vesicles." *Advanced Drug Delivery Reviews* 159: 308–321.

Sun, Y., G. Liu, K. Zhang, Q. Cao, T. Liu, and J. Li. 2021. "Mesenchymal Stem Cells-Derived Exosomes for Drug Delivery." *Stem Cell Research & Therapy* 12, no. 1: 1–15.

Tammaro, O., A. C. di Polidoro, E. Romano, P. A. Netti, and E. Torino. 2020. "A Microfluidic Platform to Design Multimodal Peg-Crosslinked Hyaluronic Acid Nanoparticles (Peg-Chanps) for Diagnostic Applications." *Scientific Reports* 10, no. 1: 1–11.

Thakur, A., R. K. Sidu, H. Zou, M. K. Alam, M. Yang, and Y. Lee. 2020. "Inhibition of Glioma Cells' Proliferation by Doxorubicin-Loaded Exosomes via Microfluidics." *International Journal of Nanomedicine* 15: 8331.

Tian, Y., S. Li, J. Song, et al. 2014. "A Doxorubicin Delivery Platform Using Engineered Natural Membrane Vesicle Exosomes for Targeted Tumor Therapy." *Biomaterials* 35, no. 7: 2383–2390.

Toderascu, L. I., L. E. Sima, S. Orobeti, et al. 2023. "Synthesis and Anti-Melanoma Activity of L-Cysteine-Coated Iron Oxide Nanoparticles Loaded With Doxorubicin." *Nanomaterials* 13, no. 4: 621.

Tomasoni, S., L. Longaretti, C. Rota, et al. 2013. "Transfer of Growth Factor Receptor Mrna Via Exosomes Unravels the Regenerative Effect of Mesenchymal Stem Cells." *Stem Cells and Development* 22, no. 5: 772–780.

Tong, Q., K. Li, F. Huang, et al. 2023. "Extracellular Vesicles Hybrid Plasmid-Loaded Lipid Nanovesicles for Synergistic Cancer Immunotherapy." *Materials Today Bio* 23: 100845.

Trucco, M. M., C. F. Meyer, K. A. Thornton, et al. 2018. "A Phase Ii Study of Temsirolimus and Liposomal Doxorubicin for Patients With Recurrent and Refractory Bone and Soft Tissue Sarcomas." *Clinical Sarcoma Research* 8, no. 1: 21.

Tudor, M., R. C. Popescu, R. D. Negoita, et al. 2023. "In vitro Hyperspectral Biomarkers of Human Chondrosarcoma Cells in Nanoparticle-Mediated Radiosensitization Using Carbon Ions." *Scientific Reports* 13: 14878. https://doi.org/10.1038/s41598-023-41991-9.

Vader, P., E. A. Mol, G. Pasterkamp, and R. M. Schiffelers. 2016. "Extracellular Vesicles for Drug Delivery." *Advanced Drug Delivery Reviews* 106: 148–156.

Wang, N., C. Chen, D. Yang, et al. 2017. "Mesenchymal Stem Cells-Derived Extracellular Vesicles, via miR-210, Improve Infarcted Cardiac Function By Promotion of Angiogenesis." *Biochimica et Biophysica Acta (BBA)-Molecular Basis of Disease* 1863, no. 8: 2085–2092.

Wei, H., F. Chen, J. Chen, et al. 2022. "Mesenchymal Stem Cell Derived Exosomes as Nanodrug Carrier of Doxorubicin for Targeted Osteosarcoma Therapy via SDF1-CXCR4 Axis." *International Journal of Nanomedicine* 17: 3483–3495.

Wei, H., J. Chen, S. Wang, et al. 2019. "A Nanodrug Consisting of Doxorubicin and Exosome Derived From Mesenchymal Stem Cells for Osteosarcoma Treatment in Vitro." *International Journal of Nanomedicine* 14: 8603.

Weigelt, B., C. M. Ghajar, and M. J. Bissell. 2014. "The Need for Complex 3D Culture Models to Unravel Novel Pathways and Identify Accurate Biomarkers in Breast Cancer." *Advanced Drug Delivery Reviews* 69–70: 42–51.

Xin, H., Y. Li, Y. Cui, J. J. Yang, Z. G. Zhang, and M. Chopp. 2013a. "Systemic Administration of Exosomes Released From Mesenchymal Stromal Cells Promote Functional Recovery and Neurovascular Plasticity after Stroke in Rats." *Journal of Cerebral Blood Flow and Metabolism: Official Journal of the International Society of Cerebral Blood Flow and Metabolism* 33, no. 11: 1711–1715.

Xin, H., Y. Li, Z. Liu, et al. 2013b. "MiR-133b Promotes Neural Plasticity and Functional Recovery After Treatment of Stroke With Multipotent Mesenchymal Stromal Cells in Rats via Transfer of Exosome-Enriched Extracellular Particles." *Stem Cells* 31, no. 12: 2737–2746.

Yan, Z., T. Zhang, Y. Wang, S. Xiao, and J. Gao. 2023. "Extracellular Vesicle Biopotentiated Hydrogels for Diabetic Wound Healing: The Art of Living Nanomaterials Combined With Soft Scaffolds." *Materials Today Bio* 23: 100810.

Yu, B., M. Gong, Y. Wang, et al. 2013. "Cardiomyocyte Protection by GATA-4 Gene Engineered Mesenchymal Stem Cells is Partially Mediated by Translocation of miR-221 in Microvesicles." *PLoS One* 8, no. 8: e73304.

Zając, A. E., S. Kopeć, B. Szostakowski, et al. 2021. "Chondrosarcoma-From Molecular Pathology to Novel Therapies." *Cancers* 13, no. 10: 2390.

Zhang, Y., S. Madabhushi, T. Tang, et al. 2024. "Contributions of Chinese Hamster Ovary Cell Derived Extracellular Vesicles and Other Cellular Materials to Hollow Fiber Filter Fouling During Perfusion Manufacturing of Monoclonal Antibodies." *Biotechnology and Bioengineering* 121: 1674–1687.

Supporting Information

Additional supporting information can be found online in the Supporting Information section.

10970290, 0, Downloaded from https://analyticalsciencejournals.onlinelibrary.wiley.com/doi/10.1002/bit.28969 by Enza Torino - Uni Federico II Di Napoli , Wiley Online Library on [19/12/2024]. See the Terms and Conditions (https://onlinelibrary.wiley.com/terms-and-conditions) on Wiley Online Library for rules of use; OA articles are governed by the applicable Creative Commons License